ISSN 1726-5479

SENSORS & TRANSDUCERS

vol. 108
9/09

TEDS Sensors, IEEE 1451 Standards

International Frequency Sensor Association Publishing

Sensors & Transducers

Volume 108, Issue 9
September 2009

www.sensorsportal.com

ISSN 1726-5479

Editors-in-Chief: professor Sergey Y. Yurish,
Phone: +34 696067716, fax: +34 93 4011989, e-mail: editor@sensorsportal.com

Editors for Western Europe
Meijer, Gerard C.M., Delft University of Technology, The Netherlands
Ferrari, Vittorio, Universitá di Brescia, Italy

Editor South America
Costa-Felix, Rodrigo, Inmetro, Brazil

Editor for Eastern Europe
Sachenko, Anatoly, Ternopil State Economic University, Ukraine

Editors for North America
Datskos, Panos G., Oak Ridge National Laboratory, USA
Fabien, J. Josse, Marquette University, USA
Katz, Evgeny, Clarkson University, USA

Editor for Asia
Ohyama, Shinji, Tokyo Institute of Technology, Japan

Editor for Asia-Pacific
Mukhopadhyay, Subhas, Massey University, New Zealand

Editorial Advisory Board

Abdul Rahim, Ruzairi, Universiti Teknologi, Malaysia
Ahmad, Mohd Noor, Nothern University of Engineering, Malaysia
Annamalai, Karthigeyan, National Institute of Advanced Industrial Science and Technology, Japan
Arcega, Francisco, University of Zaragoza, Spain
Arguel, Philippe, CNRS, France
Ahn, Jae-Pyoung, Korea Institute of Science and Technology, Korea
Arndt, Michael, Robert Bosch GmbH, Germany
Ascoli, Giorgio, George Mason University, USA
Atalay, Selcuk, Inonu University, Turkey
Atghiaee, Ahmad, University of Tehran, Iran
Augutis, Vygantas, Kaunas University of Technology, Lithuania
Avachit, Patil Lalchand, North Maharashtra University, India
Ayesh, Aladdin, De Montfort University, UK
Bahreyni, Behraad, University of Manitoba, Canada
Baliga, Shankar, B., General Monitors Transnational, USA
Baoxian, Ye, Zhengzhou University, China
Barford, Lee, Agilent Laboratories, USA
Barlingay, Ravindra, RF Arrays Systems, India
Basu, Sukumar, Jadavpur University, India
Beck, Stephen, University of Sheffield, UK
Ben Bouzid, Sihem, Institut National de Recherche Scientifique, Tunisia
Benachaiba, Chellali, Universitaire de Bechar, Algeria
Binnie, T. David, Napier University, UK
Bischoff, Gerlinde, Inst. Analytical Chemistry, Germany
Bodas, Dhananjay, IMTEK, Germany
Borges Carval, Nuno, Universidade de Aveiro, Portugal
Bousbia-Salah, Mounir, University of Annaba, Algeria
Bouvet, Marcel, CNRS – UPMC, France
Brudzewski, Kazimierz, Warsaw University of Technology, Poland
Cai, Chenxin, Nanjing Normal University, China
Cai, Qingyun, Hunan University, China
Campanella, Luigi, University La Sapienza, Italy
Carvalho, Vitor, Minho University, Portugal
Cecelja, Franjo, Brunel University, London, UK
Cerda Belmonte, Judith, Imperial College London, UK
Chakrabarty, Chandan Kumar, Universiti Tenaga Nasional, Malaysia
Chakravorty, Dipankar, Association for the Cultivation of Science, India
Changhai, Ru, Harbin Engineering University, China
Chaudhari, Gajanan, Shri Shivaji Science College, India
Chavali, Murthy, VIT University, Tamil Nadu, India
Chen, Jiming, Zhejiang University, China
Chen, Rongshun, National Tsing Hua University, Taiwan
Cheng, Kuo-Sheng, National Cheng Kung University, Taiwan
Chiang, Jeffrey (Cheng-Ta), Industrial Technol. Research Institute, Taiwan
Chiriac, Horia, National Institute of Research and Development, Romania
Chowdhuri, Arijit, University of Delhi, India
Chung, Wen-Yaw, Chung Yuan Christian University, Taiwan
Corres, Jesus, Universidad Publica de Navarra, Spain
Cortes, Camilo A., Universidad Nacional de Colombia, Colombia
Courtois, Christian, Universite de Valenciennes, France
Cusano, Andrea, University of Sannio, Italy
D'Amico, Arnaldo, Università di Tor Vergata, Italy
De Stefano, Luca, Institute for Microelectronics and Microsystem, Italy
Deshmukh, Kiran, Shri Shivaji Mahavidyalaya, Barshi, India
Dickert, Franz L., Vienna University, Austria
Dieguez, Angel, University of Barcelona, Spain
Dimitropoulos, Panos, University of Thessaly, Greece
Ding, Jianning, Jiangsu Polytechnic University, China
Djordjevich, Alexandar, City University of Hong Kong, Hong Kong
Donato, Nicola, University of Messina, Italy
Donato, Patricio, Universidad de Mar del Plata, Argentina
Dong, Feng, Tianjin University, China
Drljaca, Predrag, Instersema Sensoric SA, Switzerland
Dubey, Venketesh, Bournemouth University, UK
Enderle, Stefan, Univ.of Ulm and KTB Mechatronics GmbH, Germany
Erdem, Gursan K. Arzum, Ege University, Turkey
Erkmen, Aydan M., Middle East Technical University, Turkey
Estelle, Patrice, Insa Rennes, France
Estrada, Horacio, University of North Carolina, USA
Faiz, Adil, INSA Lyon, France
Fericean, Sorin, Balluff GmbH, Germany
Fernandes, Joana M., University of Porto, Portugal
Francioso, Luca, CNR-IMM Institute for Microelectronics and Microsystems, Italy
Francis, Laurent, University Catholique de Louvain, Belgium
Fu, Weiling, South-Western Hospital, Chongqing, China
Gaura, Elena, Coventry University, UK
Geng, Yanfeng, China University of Petroleum, China
Gole, James, Georgia Institute of Technology, USA
Gong, Hao, National University of Singapore, Singapore
Gonzalez de la Rosa, Juan Jose, University of Cadiz, Spain
Granel, Annette, Goteborg University, Sweden
Graff, Mason, The University of Texas at Arlington, USA
Guan, Shan, Eastman Kodak, USA
Guillet, Bruno, University of Caen, France
Guo, Zhen, New Jersey Institute of Technology, USA
Gupta, Narendra Kumar, Napier University, UK
Hadjiloucas, Sillas, The University of Reading, UK
Haider, Mohammad R., Sonoma State University, USA
Hashsham, Syed, Michigan State University, USA
Hasni, Abdelhafid, Bechar University, Algeria
Hernandez, Alvaro, University of Alcala, Spain
Hernandez, Wilmar, Universidad Politecnica de Madrid, Spain
Homentcovschi, Dorel, SUNY Binghamton, USA
Horstman, Tom, U.S. Automation Group, LLC, USA
Hsiai, Tzung (John), University of Southern California, USA
Huang, Jeng-Sheng, Chung Yuan Christian University, Taiwan
Huang, Star, National Tsing Hua University, Taiwan
Huang, Wei, PSG Design Center, USA
Hui, David, University of New Orleans, USA
Jaffrezic-Renault, Nicole, Ecole Centrale de Lyon, France
Jaime Calvo-Galleg, Jaime, Universidad de Salamanca, Spain
James, Daniel, Griffith University, Australia
Janting, Jakob, DELTA Danish Electronics, Denmark
Jiang, Liudi, University of Southampton, UK
Jiang, Wei, University of Virginia, USA
Jiao, Zheng, Shanghai University, China
John, Joachim, IMEC, Belgium
Kalach, Andrew, Voronezh Institute of Ministry of Interior, Russia
Kang, Moonho, Sunmoon University, Korea South
Kaniusas, Eugenijus, Vienna University of Technology, Austria
Katake, Anup, Texas A&M University, USA
Kausel, Wilfried, University of Music, Vienna, Austria
Kavasoglu, Nese, Mugla University, Turkey
Ke, Cathy, Tyndall National Institute, Ireland
Khan, Asif, Aligarh Muslim University, Aligarh, India
Sapozhnikova, Ksenia, D.I.Mendeleyev Institute for Metrology, Russia

Kim, Min Young, Kyungpook National University, Korea South
Ko, Sang Choon, Electronics and Telecommunications Research Institute, Korea South
Kockar, Hakan, Balikesir University, Turkey
Kotulska, Malgorzata, Wroclaw University of Technology, Poland
Kratz, Henrik, Uppsala University, Sweden
Kumar, Arun, University of South Florida, USA
Kumar, Subodh, National Physical Laboratory, India
Kung, Chih-Hsien, Chang-Jung Christian University, Taiwan
Lacnjevac, Caslav, University of Belgrade, Serbia
Lay-Ekuakille, Aime, University of Lecce, Italy
Lee, Jang Myung, Pusan National University, Korea South
Lee, Jun Su, Amkor Technology, Inc. South Korea
Lei, Hua, National Starch and Chemical Company, USA
Li, Genxi, Nanjing University, China
Li, Hui, Shanghai Jiaotong University, China
Li, Xian-Fang, Central South University, China
Liang, Yuanchang, University of Washington, USA
Liawruangrath, Saisunee, Chiang Mai University, Thailand
Liew, Kim Meow, City University of Hong Kong, Hong Kong
Lin, Hermann, National Kaohsiung University, Taiwan
Lin, Paul, Cleveland State University, USA
Linderholm, Pontus, EPFL - Microsystems Laboratory, Switzerland
Liu, Aihua, University of Oklahoma, USA
Liu Changgeng, Louisiana State University, USA
Liu, Cheng-Hsien, National Tsing Hua University, Taiwan
Liu, Songqin, Southeast University, China
Lodeiro, Carlos, Universidade NOVA de Lisboa, Portugal
Lorenzo, Maria Encarnacio, Universidad Autonoma de Madrid, Spain
Lukaszewicz, Jerzy Pawel, Nicholas Copernicus University, Poland
Ma, Zhanfang, Northeast Normal University, China
Majstorovic, Vidosav, University of Belgrade, Serbia
Marquez, Alfredo, Centro de Investigacion en Materiales Avanzados, Mexico
Matay, Ladislav, Slovak Academy of Sciences, Slovakia
Mathur, Prafull, National Physical Laboratory, India
Maurya, D.K., Institute of Materials Research and Engineering, Singapore
Mekid, Samir, University of Manchester, UK
Melnyk, Ivan, Photon Control Inc., Canada
Mendes, Paulo, University of Minho, Portugal
Mennell, Julie, Northumbria University, UK
Mi, Bin, Boston Scientific Corporation, USA
Minas, Graca, University of Minho, Portugal
Moghavvemi, Mahmoud, University of Malaya, Malaysia
Mohammadi, Mohammad-Reza, University of Cambridge, UK
Molina Flores, Esteban, Benemérita Universidad Autónoma de Puebla, Mexico
Moradi, Majid, University of Kerman, Iran
Morello, Rosario, University "Mediterranea" of Reggio Calabria, Italy
Mounir, Ben Ali, University of Sousse, Tunisia
Mulla, Imtiaz Sirajuddin, National Chemical Laboratory, Pune, India
Neelamegam, Periasamy, Sastra Deemed University, India
Neshkova, Milka, Bulgarian Academy of Sciences, Bulgaria
Oberhammer, Joachim, Royal Institute of Technology, Sweden
Ould Lahoucine, Cherif, University of Guelma, Algeria
Pamidighanta, Sayanu, Bharat Electronics Limited (BEL), India
Pan, Jisheng, Institute of Materials Research & Engineering, Singapore
Park, Joon-Shik, Korea Electronics Technology Institute, Korea South
Penza, Michele, ENEA C.R., Italy
Pereira, Jose Miguel, Instituto Politecnico de Setebal, Portugal
Petsev, Dimiter, University of New Mexico, USA
Pogacnik, Lea, University of Ljubljana, Slovenia
Post, Michael, National Research Council, Canada
Prance, Robert, University of Sussex, UK
Prasad, Ambika, Gulbarga University, India
Prateepasen, Asa, Kingmoungut's University of Technology, Thailand
Pullini, Daniele, Centro Ricerche FIAT, Italy
Pumera, Martin, National Institute for Materials Science, Japan
Radhakrishnan, S. National Chemical Laboratory, Pune, India
Rajanna, K., Indian Institute of Science, India
Ramadan, Qasem, Institute of Microelectronics, Singapore
Rao, Basuthkar, Tata Inst. of Fundamental Research, India
Raoof, Kosai, Joseph Fourier University of Grenoble, France
Reig, Candid, University of Valencia, Spain
Restivo, Maria Teresa, University of Porto, Portugal
Robert, Michel, University Henri Poincare, France
Rezazadeh, Ghader, Urmia University, Iran
Royo, Santiago, Universitat Politecnica de Catalunya, Spain
Rodriguez, Angel, Universidad Politecnica de Cataluna, Spain
Rothberg, Steve, Loughborough University, UK
Sadana, Ajit, University of Mississippi, USA
Sadeghian Marnani, Hamed, TU Delft, The Netherlands
Sandacci, Serghei, Sensor Technology Ltd., UK
Saxena, Vibha, Bhbha Atomic Research Centre, Mumbai, India
Schneider, John K., Ultra-Scan Corporation, USA
Seif, Selemani, Alabama A & M University, USA
Seifter, Achim, Los Alamos National Laboratory, USA
Sengupta, Deepak, Advance Bio-Photonics, India
Shearwood, Christopher, Nanyang Technological University, Singapore
Shin, Kyuho, Samsung Advanced Institute of Technology, Korea
Shmaliy, Yuriy, Kharkiv National Univ. of Radio Electronics, Ukraine
Silva Girao, Pedro, Technical University of Lisbon, Portugal
Singh, V. R., National Physical Laboratory, India
Slomovitz, Daniel, UTE, Uruguay
Smith, Martin, Open University, UK
Soleymanpour, Ahmad, Damghan Basic Science University, Iran
Somani, Prakash R., Centre for Materials for Electronics Technol., India
Srinivas, Talabattula, Indian Institute of Science, Bangalore, India
Srivastava, Arvind K., Northwestern University, USA
Stefan-van Staden, Raluca-Ioana, University of Pretoria, South Africa
Sumriddetchka, Sarun, National Electronics and Computer Technology Center, Thailand
Sun, Chengliang, Polytechnic University, Hong-Kong
Sun, Dongming, Jilin University, China
Sun, Junhua, Beijing University of Aeronautics and Astronautics, China
Sun, Zhiqiang, Central South University, China
Suri, C. Raman, Institute of Microbial Technology, India
Sysoev, Victor, Saratov State Technical University, Russia
Szewczyk, Roman, Industrial Research Inst. for Automation and Measurement, Poland
Tan, Ooi Kiang, Nanyang Technological University, Singapore,
Tang, Dianping, Southwest University, China
Tang, Jaw-Luen, National Chung Cheng University, Taiwan
Teker, Kasif, Frostburg State University, USA
Thumbavanam Pad, Kartik, Carnegie Mellon University, USA
Tian, Gui Yun, University of Newcastle, UK
Tsiantos, Vassilios, Technological Educational Institute of Kaval, Greece
Tsigara, Anna, National Hellenic Research Foundation, Greece
Twomey, Karen, University College Cork, Ireland
Valente, Antonio, University, Vila Real, - U.T.A.D., Portugal
Vaseashta, Ashok, Marshall University, USA
Vazquez, Carmen, Carlos III University in Madrid, Spain
Vieira, Manuela, Instituto Superior de Engenharia de Lisboa, Portugal
Vigna, Benedetto, STMicroelectronics, Italy
Vrba, Radimir, Brno University of Technology, Czech Republic
Wandelt, Barbara, Technical University of Lodz, Poland
Wang, Jiangping, Xi'an Shiyou University, China
Wang, Kedong, Beihang University, China
Wang, Liang, Advanced Micro Devices, USA
Wang, Mi, University of Leeds, UK
Wang, Shinn-Fwu, Ching Yun University, Taiwan
Wang, Wei-Chih, University of Washington, USA
Wang, Wensheng, University of Pennsylvania, USA
Watson, Steven, Center for NanoSpace Technologies Inc., USA
Weiping, Yan, Dalian University of Technology, China
Wells, Stephen, Southern Company Services, USA
Wolkenberg, Andrzej, Institute of Electron Technology, Poland
Woods, R. Clive, Louisiana State University, USA
Wu, DerHo, National Pingtung Univ. of Science and Technology, Taiwan
Wu, Zhaoyang, Hunan University, China
Xiu Tao, Ge, Chuzhou University, China
Xu, Lisheng, The Chinese University of Hong Kong, Hong Kong
Xu, Tao, University of California, Irvine, USA
Yang, Dongfang, National Research Council, Canada
Yang, Wuqiang, The University of Manchester, UK
Yang, Xiaoling, University of Georgia, Athens, GA, USA
Yaping Dan, Harvard University, USA
Ymeti, Aurel, University of Twente, Netherland
Yong Zhao, Northeastern University, China
Yu, Haihu, Wuhan University of Technology, China
Yuan, Yong, Massey University, New Zealand
Yufera Garcia, Alberto, Seville University, Spain
Zagnoni, Michele, University of Southampton, UK
Zamani, Cyrus, Universitat de Barcelona, Spain
Zeni, Luigi, Second University of Naples, Italy
Zhang, Minglong, Shanghai University, China
Zhang, Qintao, University of California at Berkeley, USA
Zhang, Weiping, Shanghai Jiao Tong University, China
Zhang, Wenming, Shanghai Jiao Tong University, China
Zhang, Xueji, World Precision Instruments, Inc., USA
Zhong, Haoxiang, Henan Normal University, China
Zhu, Qing, Fujifilm Dimatix, Inc., USA
Zorzano, Luis, Universidad de La Rioja, Spain
Zourob, Mohammed, University of Cambridge, UK

Sensors & Transducers Journal (ISSN 1726-5479) is a peer review international journal published monthly online by International Frequency Sensor Association (IFSA).
Available in electronic and on CD. Copyright © 2009 by International Frequency Sensor Association. All rights reserved.

Sensors & Transducers Journal

Contents

Volume 108
Issue 9
September 2009

www.sensorsportal.com

ISSN 1726-5479

Research Articles

Smart Sensor for Analyzing Train Vibration in WCR Zone
Alka Dubey and Ashish Verma 1

Design of a Low Cost Smart Dryer Temperature Measurement System for Tea Factories
Utpal Sarma, Digbijoy Chakraborty, Pradip Kr. Boruah 8

Design of a MEMS Capacitive Comb-drive Micro-accelerometer with Sag Optimization
B. D. Pant, Lokesh Dhakar, P. J. George and S. Ahmad 15

Dynamic Characterization of MEMS Scanners
Çağlar Ataman, Hüseyin R. Seren, Harald Schenk, Hakan Ürey 31

Electromagnetic Investigation of a CMOS MEMS Inductive Microphone
Farès Tounsi, Brahim Mezghani, Libor Rufer, Mohamed Masmoudi and Salvador Mir. 40

Study of Thermoelastic Damping in Capacitive Micro-beam Resonators Using Hyperbolic Heat Conduction Model
Ghader Rezazadeh, Armin Saeedi vahdat, Seyed-Mehdi Pesteii,Bahman Farzi 54

Development of Planter Foot Pressure Distribution System Using Flexi Force Sensors
S. L. Patil, Madhuri A. Thatte, U. M. Chaskar 73

Fiber Optic Displacement and Liquid Refractive Index Sensors with Two Asymmetrical Inclined Fibers
H. Z. Yang, S. W. Harun and H. Ahmad 80

Controlling a pH Process Using Feedback & Double Controller Scheme
S. Shobana, A. Srinivasan and Rames C. Panda 89

Time Domain Analysis of Ultrasonic Wave Propagation using an Electromagnetic Acoustic Transducer
Sadiq Thomas, Salah Obayya, Domenico Pinto, D. Dulay, W. Balachandran, Mostafa Darwish 102

Design of a PC Based Mass Flow Indicator of an Electrical Motor Driven Water Lift Pump using Motor Load Current as the Flow Sensing Parameter
S. C. Bera, N. Mandal and R. Sarkar. 116

A Bimorph Moment/Force Actuator for Dynamic Testing
Hou Xiaoyan 128

Instrumentation to Measure the Capacitance of Biosensors by Sinusoidal Wave Method
Pavan Kumar Kathuroju and Nagaraju Jampana 139

Humidity and Electrical Sensing Properties of $CoCr_2O_4$–ZnO–MnO_2 Composites
Regina Mary L., Jeyaraj B. and Nagaraja K. S. 147

AC Response to Humidity and Propane of Sprayed Fe-Zn Oxide Films
Alejandro Avila-García, Manuel García-Hipólito and Yasuhiro Matsumoto-Kuwabara...................... 156

Sn-doped Zinc Oxide Thin Films for Methanol
Rajarshi Krishna Nath and Siddhartha Sankar Nath... 168

Spray Deposited Pure and CuO Doped ZnO Thin Films for NH_3 Sensing
L. A. Patil, I. G. Pathan.. 180

Formulation and Characterization of Cr_2O_3 Doped ZnO Thick Films as H_2S Gas Sensor
A. V. Patil, C. G. Dighavkar, S. K. Sonawane, S. J. Patil and R. Y. Borse....................................... 189

Authors are encouraged to submit article in MS Word (doc) and Acrobat (pdf) formats by e-mail: editor@sensorsportal.com
Please visit journal's webpage with preparation instructions: http://www.sensorsportal.com/HTML/DIGEST/Submition.htm

Sensors & Transducers Journal, Vol. 108, Issue 9, September 2009, pp. 40-53

www.sensorsportal.com

Sensors & Transducers

ISSN 1726-5479
© 2009 by IFSA
http://www.sensorsportal.com

Electromagnetic Investigation of a CMOS MEMS Inductive Microphone

[1,2] Farès TOUNSI, [1] Brahim MEZGHANI, [2] Libor RUFER, [1] Mohamed MASMOUDI and [2] Salvador MIR

[1]Electronics, Microtechnology and Communication (EMC), National Engineering School of Sfax
Route Soukra, BP 1173, 3038 Sfax, Tunisia
[2]TIMA Laboratory (CNRS, G-INP, UJF)
46, Avenue Félix Viallet, 38031 Grenoble, France
Tel. :+33-476574646; fax: +33-476574981
E-mail: fares.tounsi@isimsf.rnu.tn

Received: 25 July 2009 /Accepted: 21 September 2009 /Published: 28 September 2009

Abstract: This paper presents a detailed electromagnetic modeling for a new structure of a monolithic CMOS micromachined inductive microphone. We have shown, that the use of an alternative current (AC) in the primary fixed inductor results in a substantially higher induced voltage in the secondary inductor comparing to the case when a direct current (DC) is used. The expected increase of the induced voltage can be expressed by a voltage ratio of AC and DC solutions that is in the range of 3 to 6. A prototype fabrication of this microphone has been realized using a combination of standard CMOS 0.6 μm process with a CMOS-compatible post-process consisting in a bulk micromachining technology. The output voltage of the electrodynamic microphone that achieves the μV range can be increased by the use of the symmetric dual-layer spiral inductor structure. *Copyright © 2009 IFSA.*

Keywords: MEMS, Electromagnetic modeling, inductive microphone, micromachined inductors, induced voltage.

1. Introduction

A microphone is an electroacoustic transducer that converts pressure inputs into an electrical signal and is widely employed in numerous applications from different fields as consumer, industrial [1], health [2], and others [3]. A variety of transduction schemes, such as piezoresistive, piezoelectric,

electrostatic, or optical have been used for acousto-electrical conversion. The vast majority of microphones are designed for audio applications, including a bandwidth less than 20 kHz and a maximum pressure less than 120 dB (ref. to 20 μPa).

Among various designs, piezoresistive microphones have the advantages of simple fabrication processes and integration into semiconductor devices [4]. It uses materials and processes to make gauges that can be integrated on beams or membranes. The electrical resistivity of these gauges changes with the variation of mechanical stress produced by deflection caused by sound waves. Piezoelectric microphones can have a similar design as piezoresistives ones, but the materials used for these devices generate differences in electrical charge at the surface instead of changing resistivity. However, piezoelectric systems suffer from both low sensitivity and the requirement to utilize specific piezo-materials such as ZnO, A1N, PVDF and PZT that need a non standard fabrication process [5].

Another effect, widely used in microphones, is the electrostatic transduction. Microphones employing this effect, called electrostatic or capacitive, are sensitive to variations in an electrostatic field created between two electrodes. This variation is induced by the movement of a microphone membrane due to the acoustic pressure. The electrical field, necessary for the microphone operation can be either supplied by an external source or created by a deposition of a material layer that can quasi-permanently keep the electrical charge between the two electrodes. This material, called electret, brings the potential for the use in portable applications [6]. Capacitive microphones have many advantages such as a relatively high sensitivity, a large bandwidth, inherently low power consumption and a low noise floor. However, in the design of capacitive microphones, specific issues such as electrostatic pull-in instability, output signal attenuation due to the parasitic capacitance and in certain designs, a decreased sensitivity at high frequencies due to the viscous damping of the perforated backplate must be solved [7]. Moreover, if an electret microphone is considered for an integration using MEMS technology, low quality of thin film electrets and charge loss due to humidity are limiting factors. The problem of detecting a small capacitance change has been overcome by clever preamplifier designs. However, narrow mechanical and electronic component tolerances have kept the price of condenser microphones relatively high.

Optical detection is another alternative to detect sound pressure. The idea of an optical microphone is based on the modulation of light rather than the conversion from an existing energy form into light energy [8]. Optical interferometric microphones have, theoretically, a dynamic range and sensitivity comparable to or better than capacitive sensors, depending on the available source power [9]. Optical microphones have the advantage that they can be deployed in harsh environments and are immune from electromagnetic interference; however, they require a stable light source and complex packaging [10].

To overcome problems related to the microphone integration, a more flexible approach is presented in this work. We have shown in our previous work the feasibility of an inductive micromachined single-wafer silicon microphone [11, 12, 16]. The monolithic integration with the electronics using a standard CMOS 0.6μm micromachining process was presented. This monolithic integration will increase performances, miniaturize the system, increase the sensitivity and in particular decrease noise, due to the reduction of interconnections parasitic capacitance. Furthermore, our approach focuses on low-cost MEMS microphone obtained by processing chips issued from an industrial standard CMOS process. In this approach, we use silicon and other layers issued from a CMOS process as basic materials for the mechanical part of the system.

2. Operation Mode of the Microphone

The structure of the electrodynamic microphone, made with a standard CMOS technology, is shown in Fig. 1. The microphone consists mainly of two inductors which occupy separate regions. The first one, a stationary outer inductor L_1, is placed on top of the substrate and an inner inductor L_2 is fabricated on top of a flexible plate suspended over the micromachined cavity. This square plate, attached to the substrate with four arms, one at each corner, has a role of the microphone sensitive part (membrane). The electromagnetic field necessary for the microphone function can be created by an electrical current flowing through one or both inductors. This polarization current can be either direct (DC) or alternative (AC). Thus, a variable magnetic field in space and/or in time will be generated in the vicinity of the inner inductor L_2 that will move due to the movement of the suspended membrane under the incident acoustic energy. According to Faraday's law, the vibration of the inductor L_2 in a magnetic field will generate at its ends an electromotive force (*emf*), proportional to the amplitude of the incident acoustic pressure. This voltage will be processed by the electronic circuitry integrated on the same chip.

The cavity under the suspended membrane is obtained using the front-side bulk micromachining realized after an industrial CMOS process, with no modification in the standard IC fabrication, no additional masking and no negative effects on the associated electronic parts. In this back-end process, a part of the bulk silicon material is etched through openings patterned in dielectric and passivation layers. These openings are easily constructed along with the suspended membrane and the attachments arms through the appropriate placement of open areas in the layout. Nevertheless, design rules of a given technology process must be respected, which defines the minimum open area width (5 µm in our case).

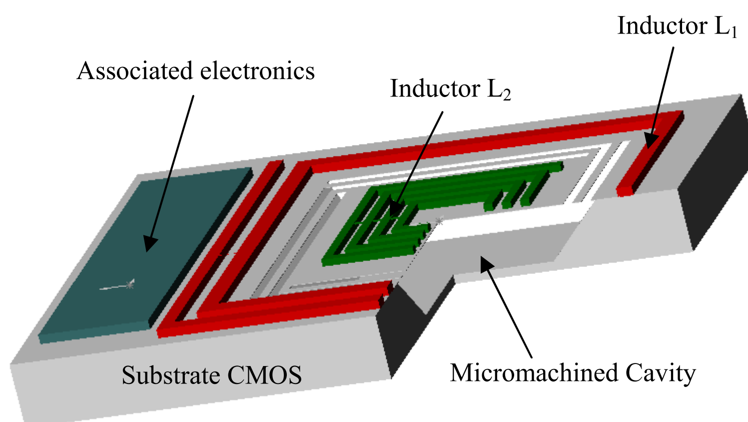

Fig. 1. Structure of the electrodynamic microphone.

3. Induced Electromotive Force (emf)

The magnetic field (B-field), at any point P in the space, produced by straight wire carrying current I is given by Biot-Savart law as shown in the following equation:

$$B_z = \frac{\mu_0}{4\pi}\frac{I}{r}\left(\sin\theta_1 + \sin\theta_2\right), \tag{1}$$

where μ_0 is the magnetic permeability of the air, r is the perpendicular distance separating P from the wire, and θ_1, θ_2 are the angles shown in Fig. 2 (a).

Circuits having a rectangular shape are made of straight segments and the B-field of such circuits can be obtained by adding their separate contributions. Thus, for a squared loop of side *a,* placed in the x-y-plane (Fig. 2 (b)), flown by a uniform current density on its four segments, will produce three magnetic field components, constant in time and nonuniform in space as given by the following set of equations [12]:

$$B_x(P) = \frac{\mu_0 I\, z}{4\pi}\left[\frac{1}{(\frac{a}{2}-x)^2+z^2}\left(\frac{\frac{a}{2}-y}{A_1}+\frac{\frac{a}{2}+y}{A_2}\right)-\frac{1}{(\frac{a}{2}+x)^2+z^2}\left(\frac{\frac{a}{2}-y}{A_3}+\frac{\frac{a}{2}+y}{A_4}\right)\right]$$

$$B_y(P) = \frac{\mu_0 I\, z}{4\pi}\left[\frac{1}{(\frac{a}{2}-y)^2+z^2}\left(\frac{\frac{a}{2}-x}{A_1}+\frac{\frac{a}{2}+x}{A_3}\right)-\frac{1}{(\frac{a}{2}+y)^2+z^2}\left(\frac{\frac{a}{2}-x}{A_2}+\frac{\frac{a}{2}+x}{A_4}\right)\right]$$

$$B_z(P) = \frac{\mu_0 I}{4\pi}\left[\frac{\frac{a}{2}+x}{(\frac{a}{2}+x)^2+z^2}\left(\frac{\frac{a}{2}-y}{A_1}+\frac{\frac{a}{2}+y}{A_2}\right)+\frac{(\frac{a}{2}-x)}{(\frac{a}{2}-x)^2+z^2}\left(\frac{\frac{a}{2}-y}{A_3}+\frac{\frac{a}{2}+y}{A_4}\right)\right.$$
$$\left.+\frac{\frac{a}{2}-y}{(\frac{a}{2}-y)^2+z^2}\left(\frac{\frac{a}{2}-x}{A_1}+\frac{\frac{a}{2}+x}{A_3}\right)+\frac{\frac{a}{2}+y}{(\frac{a}{2}+y)^2+z^2}\left(\frac{\frac{a}{2}-x}{A_2}+\frac{\frac{a}{2}+x}{A_4}\right)\right] \quad (2)$$

where, $A_1 = \sqrt{(\frac{a}{2}-x)^2+z^2+(\frac{a}{2}-y)^2}$, $A_2 = \sqrt{(\frac{a}{2}-x)^2+z^2+(\frac{a}{2}+y)^2}$,

$A_3 = \sqrt{(\frac{a}{2}+x)^2+z^2+(\frac{a}{2}-y)^2}$, $A_4 = \sqrt{(\frac{a}{2}+x)^2+z^2+(\frac{a}{2}+y)^2}$

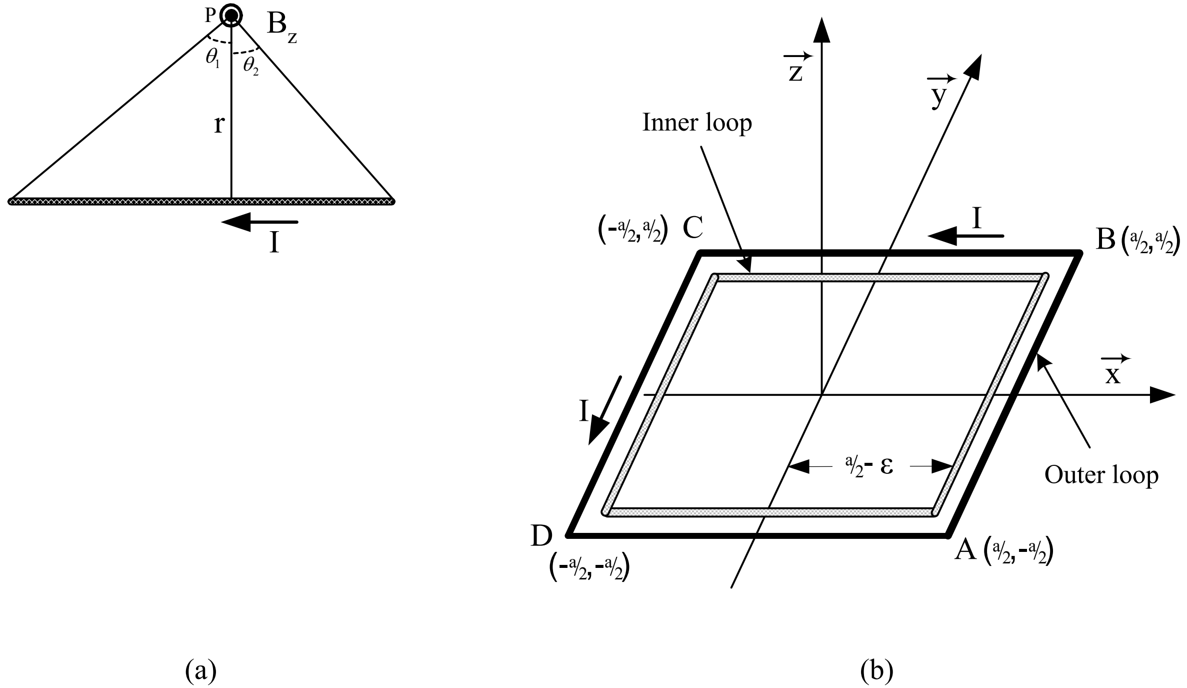

Fig. 2. Geometric relations between magnetic field and conductors in the case of: straight wire (a), and closed loops (b).

In general, the total electromotive force, as given by Faraday's law, is a voltage that arises in a closed conducting path from the time rate of change of the flux (*emf=-dΦ/dt*). A nonzero value of the *emf* may result from a relative motion between a steady flux and the closed path, Φ_c, and/or a time-changing flux linking the stationary closed path like its show by equation (3) [21].

$$emf = -\frac{d\Phi}{dt} = -\frac{d}{dt}\iint_S \vec{B}.d\vec{S} - \frac{d\Phi_c}{dt} \tag{3}$$

In the case of two inductively coupled coils, we can identify the leakage flux Φ_{22} produced by the current i_2 and the flux Φ_{21} that links both currents i_1 and i_2 like its show by equation (4)

$$\Phi = \iint_S \vec{B}.d\vec{S} = \Phi_{22} + \Phi_{21} = L_2 i_2 + M i_1 \tag{4}$$

In the following sub-sections, we will derive expressions for the induced voltage in different possible cases of polarization, depending on currents flowing in one or both inductors.

3.1. Case 1: Outer Inductor Carrying a DC Bias Current

We consider two squared loops, the outer is stationary and the inner one moves up and down along the z-axis with the deflection of the membrane caused by incident acoustic pressure. In a general case, the incident acoustic pressure is a broad-band signal. For simplicity, we will take into account, in this scalable study, only one frequency. Supposing that the membrane exercise a piston-like movement, the instantaneous inductor displacement is given by $\xi_m = h(\omega_p)\ sin(\omega_p t)$, where ω_p is the angular velocity of the incident acoustic pressure and h is the corresponding amplitude of the membrane deflection. According to Faraday's law, an induced electromotive force (*emf*) in the inner closed-loop circuit will be produced. This electromotive force, called motional *emf*, is generated by the movement of the closed conducting loop through a time-independent but spatially varying magnetic field. The expression of the emf_m is proportional to the variation of the magnetic flux, Φ_c, as given by the following equation [13]:

$$emf_m = -\frac{d\Phi_c}{dt} = \oint_{loop} \vec{E_m}.\vec{dl} = \oint_{loop} (\vec{v} \wedge \vec{B}).\vec{dl}\ , \tag{5}$$

where E_m is called the motional electric field, dl represents the elementary displacement of the loop and v is the conductor velocity given by deriving the displacement ξ_m with respect to the time. The value of the emf_m is equal to the algebraic sum of the voltage drops across each segment forming the loop. For time-constant B-fields, the emf_m is given by equation (6):

$$\begin{aligned} emf_m = h\,\omega_p\, cos(\omega_p t) \times \Bigg[& \int_{AB} \left(\vec{z} \wedge B_{x/(x=a/2-\varepsilon)}.\vec{x}\right).\,dy\vec{y} + \int_{BC} \left(\vec{z} \wedge B_{y/(y=a/2-\varepsilon)}.\vec{y}\right).\,dx\vec{x} \\ & - \int_{CD} \left(\vec{z} \wedge B_{x/(x=-a/2+\varepsilon)}.\vec{x}\right).\,dy\vec{y} - \int_{DA} \left(\vec{z} \wedge B_{y/(y=-a/2+\varepsilon)}.\vec{y}\right).\,dx\vec{x} \Bigg], \end{aligned} \tag{6}$$

where ε is the average distance separating the inner closed-loop circuit from the outer. B_x and B_y are odd functions relative to the x and y variables because of the symmetry properties of the square loop geometry. The resulting simplified expression of the emf_m is given by equation (7):

$$emf_m = 4h\omega_p\, cos(\omega_p t) \int_{-\frac{a}{2}+\varepsilon}^{\frac{a}{2}-\varepsilon} B_{x/(x=a/2-\varepsilon)}.\,dy \tag{7}$$

The accurate expression of the emf_m as a function of the z-axis displacement, ξ_m, is given by equation (8):

$$emf_m = \frac{2\mu_0 I}{\pi} \frac{\xi_m \left(\sqrt{\varepsilon^2 + \xi_m^2 + (a-\varepsilon)^2} - \sqrt{2\varepsilon^2 + \xi_m^2} \right)}{\varepsilon^2 + \xi_m^2} h\omega_p \cos(\omega_p t) = A_1 h\omega_p \cos(\omega_p t) \quad (8)$$

The A_1 factor in the expression of the emf_m given by the Equation (8) depends on the displacement ξ_m and its value is shown for given dimensions in Fig. 3. This factor can be considered as linear if displacements are sufficiently small (less than 20µm in our case (Fig. 4)). When we make a series expansion for ξ_m neighboring zero, the simplified emf_m expression, for a linear range, can be approximated by the equation (9). Accordingly, the total emf_m will remain sinusoidal if the amplitude of the displacement is restricted to this limited linear range.

$$emf_m \approx \frac{2\mu_0 I}{\pi} \frac{\sqrt{\varepsilon^2 + (a-\varepsilon)^2} - \sqrt{2\varepsilon^2}}{\varepsilon^2} \xi_m h\omega_p \cos(\omega_p t) = A_2 h\omega_p \cos(\omega_p t) \quad (9)$$

In order to extend the obtained results for simple conducting loops towards planar inductors having n_1 and n_2 turns, we need to apply the following approximations. The sum of all electromotive forces will be approximated by the equivalent average effect of n_1 segments of L_1 on n_2 segments of the inner inductor L_2. Each inductor will be represented by its average length and both inductors will be placed at the average distance. Let l_a and m_a be the length of the average spire in the outer and the inner inductor, respectively. ε_a is the average distance separating the two medium spires of the two inductors ($\varepsilon_a=(l_a-m_a)/2$). When we substitute ξ_m by $h\sin(\omega_p t)$ in equation (9) the total open-circuit output voltage is given by the following equation

$$emf_m \approx n_1 n_2 \frac{\mu_0 I}{\pi} \frac{\sqrt{\varepsilon_a^2 + (l_a-\varepsilon_a)^2} - \sqrt{2\varepsilon_a^2}}{\varepsilon_a^2} h^2 \omega_p \sin(2\omega_p t) \quad (10)$$

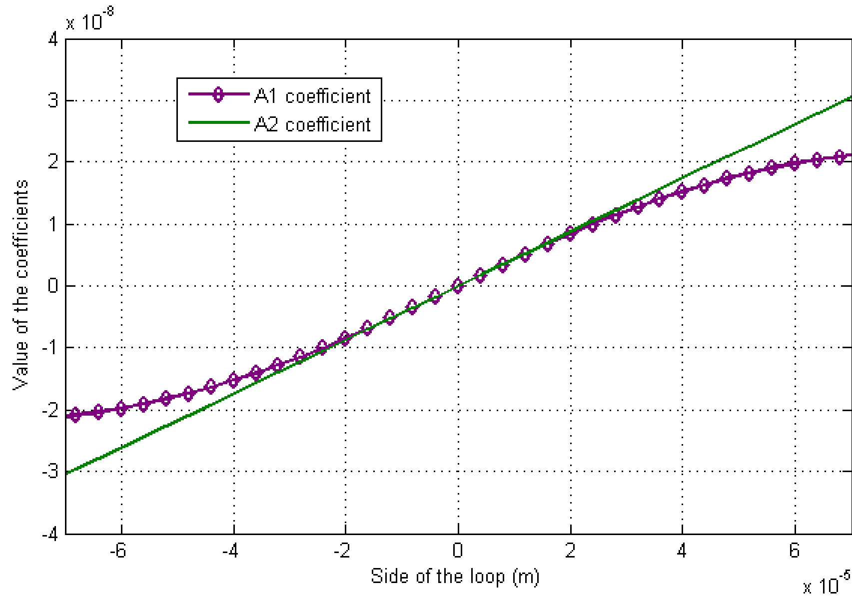

Fig. 3. Variation of the two voltage factors A_1 and A_2 of the emf_m as a function of the displacement ξ_m (for a =1.5 mm, ε=107 µm and I=5 mA).

For a medium frequency of $f_p=\omega_p/2\pi=1\ kHz$ and a maximal displacement equal to $h=10\ \mu m$, we can obtain a sinusoidal emf_m voltage in the μV range. In the final equation (10), the produced emf_m is nearly inversely proportional to the distance ε_a^2. Then, the two inductors L_1 and L_2 are required to be placed as closest as possible in order to obtain the maximal output voltage. The minimal distance is limited by the chosen technology and geometry. We can also notice that, the frequency of the output signal is doubled, compared to the incident pressure wave. This is due to the induction B_x that is an odd function of the z variable. This effect is not desirable in the microphone operation. We can reach a high voltage value if we have a large displacement but the signal includes higher harmonics. Then, we need to use filtering to recover the original signal.

3.2. Case 2: Both Inductors Carrying a DC Bias Current

In this case we consider the two inductors, inner and outer, carrying a DC bias current. This will form a tapped monolithic planar transformer illustrated in Fig. 4. The tapped transformer is actually as an inductor with a middle tap that occupies a separate region. Although it is not a symmetric design, it allows a large range of turn ratios to be realized [14, 15]. Some circuits (e.g., differential circuits) prefer transformers with a symmetrical layout. Depending on whether the lateral or vertical magnetic coupling is used, transformer structures have two categories: planar or stacked. Tapped transformer relies only on lateral magnetic coupling only. All windings can be implemented with the top metal layer, thereby minimizing terminal-to-substrate parasitic capacitances. The relationship between the secondary voltage and the primary and secondary currents is given by the following equation.

$$v_2 = \frac{dL_2 i_2}{dt} + \frac{dM i_1}{dt}, \tag{11}$$

where L_2 is the total inductance of the inner (secondary) spiral inductor and M is the mutual inductance between the segments of the inner inductor and the outer (primary) one, L_1. For a DC biasing of both inductors, equation (11) can be simplified to [16]:

$$v_2 = i_1 \frac{\partial M}{\partial t} \tag{12}$$

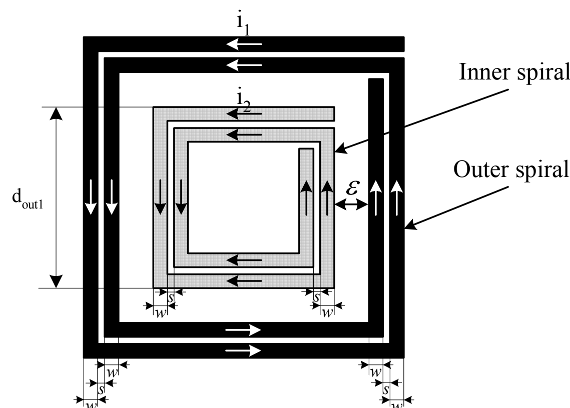

Fig. 4. Planar tapped transformer structure.

The key parameters in inductors design involve the outer dimensions, width and spacing of the metal tracks, thickness of the metal, number of turns of the spiral and the substrate material. The total

inductance of a planar spiral square inductor can be calculated according to the Greenhouse theory [17]. Basically, the spiral square inductor is split up into sections consisting of straight conductors. Then the self-inductance L_i of each section is calculated and summed up. Beside the consideration of the self-inductance of each straight conductor, the mutual inductance interaction $M_{i,j}$ (positive or negative) between the ith and j^{th} parallel segments needs to be included for the calculation of the overall inductance. Hence, supposing that each conductor includes 4 straight segments, the accurate expression of the total inductance L_1 and L_2 can be calculated using the following equation [18]:

$$L_T = \sum_{i=1}^{n} L_i + \sum_{i=1}^{n} \sum_{j=1, j \neq i}^{n} M_{i,j} \tag{13}$$

A practical approximate expression of the expression (13) can be found in [19]. The mutual inductance of two parallel conductors having the same length shown in Fig. 5-(a) is a function of this length l and of the geometric mean distance (GMD), between them. The mutual inductance parameter, M_l, is given by the following equation [17]:

$$M_l = \frac{\mu_0 l}{2\pi} \left\{ ln\left[\frac{l}{GMD} + \sqrt{1 + \frac{l^2}{GMD^2}} \right] - \sqrt{1 + \frac{GMD^2}{l^2}} + \frac{GMD}{l} \right\}, \tag{14}$$

where the *GMD* between the two conductors is approximately equal to the distance between the track center. The exact value of the GMD can be obtained from Grover's tables [29] and is given by the following equation:

$$ln(GMD) = ln(d) - \left\{ \frac{1}{12\left(\frac{d}{w}\right)^2} + \frac{1}{60\left(\frac{d}{w}\right)^4} + \frac{1}{168\left(\frac{d}{w}\right)^6} + \frac{1}{360\left(\frac{d}{w}\right)^8} + \frac{1}{660\left(\frac{d}{w}\right)^{10}} + \dots \right\}, \tag{15}$$

where d is the center to center separation between the conductors, and w is the width of the conductors. If we extend our reasoning to the configuration of the spirals in a microphone, we must take into account the instant vertical distance of both coils. The mutual inductance between both inductors spirals depends on the distance between the two surfaces of L_1 and L_2. For an inner inductor moving sinusoidally with an amplitude equal to ξ_m, the maximal distance d becomes $d=\sqrt{(\varepsilon_a^2+\xi_m^2)}$ (Fig. 5-(b)). In a planar inductor corresponding to our microphone design, we have to take into account different segment lengths as shown in Fig. 5-(c). The mutual inductance of two parallel conductors of lengths l and m, can be expressed as a difference of inductances of equal length segments, given by equation (16) [18]. Since each segments of length m are situated symmetrically with respect to the middle of length l, the expression for the mutual inductance can be written in a simplified form as:

$$M_{l,m} = M_{m+p} - M_p \tag{16}$$

To evaluate the total voltage induced in the secondary inductor due to its vertical movement, we will apply the relations obtained for the case of two rectangular conductors to the two inductors shown in Fig. 4. For the segments of the two inductors, parallel current flowing in same phase produces positive mutual inductance components, to which contribute interaction between parallel segments on the same side of a square. If the current is out-of-phase the mutual components contribution is negative, such as current in one side and the other. In our case, the negative mutual inductance can be neglected because of the large diameter of the inner inductance (range of mm). Using symmetry and noting that segments perpendicular to one another have zero mutual inductance, the total mutual inductance interactions can be approximated by an equivalent of $8n_1 \times n_2$ average interactions between segments of average length at an average distance. Taking into account these considerations and combining equations. (14), (15)

and (16), the normalized mutual inductance between two parallel concentric loops of different lengths is given by equation (17):

$$M = M_0 + \Delta M\left(\xi_m\right), \tag{17}$$

where M_0 is the normalized steady mutual inductance corresponding to the length separation between the loops of the two in-plane inductors ε_a, and $\Delta M(\xi_m)$ is the additional value of the normalized mutual inductance resulting from a distance between the two surfaces of the two inductors (see Figure 5-(b)). For values used in our design, an accurate representation of equation (17) is given in Fig. 6. The simplified terms of the mutual inductance components for small displacement can be approximated by the use of a series expansion of ξ_m, and results in:

$$M_0 \approx n_1 n_2 \frac{4\mu_0}{\pi}\left[\left(l_a - \varepsilon_a\right) ln\left(\frac{\left(l_a - \varepsilon_a\right) + \sqrt{\varepsilon_a^2 + \left(l_a - \varepsilon_a\right)^2}}{\varepsilon_a}\right) - \sqrt{\varepsilon_a^2 + \left(l_a - \varepsilon_a\right)^2} - \varepsilon_a\left(ln\left(1+\sqrt{2}\right) - \sqrt{2}\right)\right] \tag{18}$$

$$\Delta M\left(\xi_m\right) \approx n_1 n_2 \frac{2\mu_0}{\pi}\left(\frac{\sqrt{\varepsilon_a^2 + \left(l_a - \varepsilon_a\right)^2} - \sqrt{2\varepsilon_a^2}}{\varepsilon_a^2}\right)\xi_m^2 \tag{19}$$

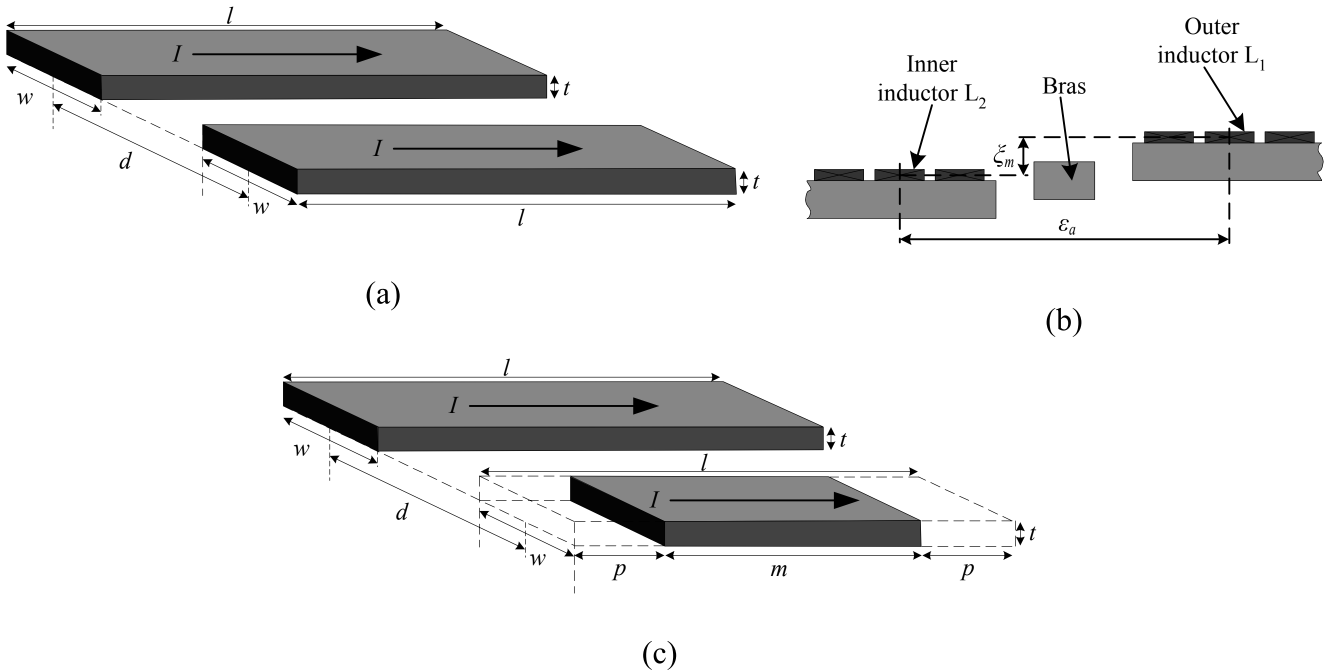

Fig. 5. Layout of two parallel-filament geometry: (a) the basic configuration (b) the situation respecting the conductor movement in a vertical direction, (c) symmetrical configuration of two segments of a different length.

The estimated expression of mutual inductance in equations (18) and (19) represent a parabolic relationship between the motion, ξ_m, of the inner inductor and the resulting mutual inductance. They widely coincide with the one in equation (17) for amplitude displacement less than 50µm (Fig. 6). We notice that, in our case, the mutual coupling coefficient M is quite small (range of µT) because of the high spatial separation, ε_a, between the two inductors.

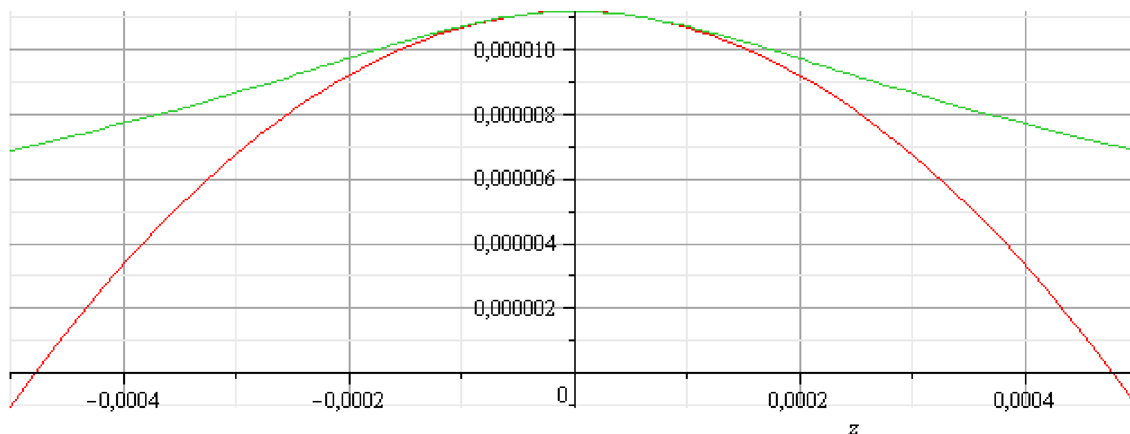

Fig. 6. Variation of the normalized mutual inductance *M* between the two inductors as a function of displacement ξ_m, with length l_a=1.5 mm, ε_a = 107 µm, thickness *w* = 0.8 µm and distance *d* = 1.0 µm.

Thus, Combining equations (12) and (17), the final expression for the normalized open-circuit output voltage of the electrodynamic microphone in the linear range can be obtained by deriving by time $\Delta M(\xi_m)$ as shown in the following equations:

$$v_2 = i_1 \frac{d\Delta M(\xi_m)}{dt} \tag{20}$$

$$v_2 \approx 2 i_1 n_1 n_2 \frac{4\mu_0}{\pi} \left(\frac{\sqrt{\varepsilon_a^2 + (l_a - \varepsilon_a)^2} - \sqrt{2\varepsilon_a^2}}{\varepsilon_a^2} \right) \xi_m \xi_m' \tag{21}$$

$$v_2 \approx 2 n_1 n_2 \frac{\mu_0 i_1}{\pi} \frac{\sqrt{\varepsilon_a^2 + (l_a - \varepsilon_a)^2} - \sqrt{2\varepsilon_a^2}}{\varepsilon_a^2} h^2 \omega_p \sin(2\omega_p t) \tag{22}$$

We can notice that the evaluated expression for the induced voltage v_2 given by the Equation (22), includes and depends on the same variable as the emf_m found in the Section 1, then, the same consequences are applied to v_2. Although, its amplitude represents the double of the emf_m, this can be explained by the mutual effect of the conductors forming the two inductors each one on the other. We can also gain more in linearity that reaches 50µm compared to the emf_m which is linear for only a *20 µm* range. For different transformer structures the mutual coupling coefficient, *k*, equal to $M/\sqrt{(L_1L_2)}$ in the tapped transformer is relatively small *(< 0.4)* [15]. Stacked transformers have a higher mutual coupling, because of the low distance between layers, but we are constrained by the operating principle and the use of standard technology in our electrodynamic microphone.

3.3. Case 3: Outer Inductor Carrying AC Bias Current

To increase the *emf* voltage produced by the acoustic pressure, we can generate a time-varying magnetic field, which will add a voltage component in the inner closed circuit. An electromotive force, as given by Faraday's law, is merely a voltage that arises from conductors moving in a constant magnetic field or a conductor submerged in a time-varying magnetic field or a combination of the two. An AC bias current applied to the outer inductor will generate a time-varying magnetic field, which

will add a voltage component in the inner closed circuit. The voltage produced by the time-varying magnetic field is called transformer action and is defined by [13]:

$$emf_t = -\frac{d\Phi}{dt} = \oint_{loop} \vec{E}.\vec{dl} = -\frac{d}{dt}\iint_S \vec{B}.d\vec{S} \ , \tag{23}$$

where S is the surface bounded by the loop formed by the spires of the inner inductor and E is the electric field. When the outer inductor is driven by an AC current, the total emf_T is given by the superposition of the two contributions defined by equations (5) and (23). The motional *emf* is a function of the velocity and the magnetic flux density, while the electromotive force induced in a stationary closed circuit is equal to the negative varying rate of the magnetic flux.

$$emf_T = \oint_{loop}\left(\vec{v}\wedge\vec{B}+\vec{E}\right)\vec{dl} = \underbrace{\oint_{loop}(\vec{v}\wedge\vec{B}).\vec{dl}}_{\text{Motional induction (generator)}} - \underbrace{\frac{d}{dt}\iint_S \vec{B}.d\vec{S}}_{\text{Transformer induction}} \tag{24}$$

In the AC configuration, the value of the current flowing through the outer inductor will be $i_1=I_0.sin(\omega_c t)$. Where, ω_c is the angular velocity. Thus, the new value of the motional *emf* will be a signal modulated in frequency and given by the following equation:

$$emf_m \approx n_1 n_2 \frac{4(\sqrt{2}-1)\mu_0 a}{\pi \varepsilon^2} I_0 \omega_p .h^2(\omega_p).sin(2\omega_p t).sin(\omega_c t) \tag{25}$$

This also can be expressed by the equation below:

$$emf_m \approx n_1 n_2 \frac{2(\sqrt{2}-1)\mu_0 a}{\pi \varepsilon^2} I_0 \omega_p .h^2.\left[cos(\omega_c t - 2\omega_p t) - cos(\omega_c t + 2\omega_p t)\right] \tag{26}$$

For the transformer induction, the corresponding *emf* will be evaluated by the following equation:

$$emf_t = -\frac{d}{dt}\iint_S B_z \, dx\, dy \tag{27}$$

To simplify the equation (27), for low amplitude displacement, supposing that B_z varies only in time and not in space, we can find a sinusoidal induced voltage of the same frequency as the has the polarization current. A series expansion neighboring zero of the *emf* can be evaluated by the following equation:

$$emf_t = -n_1 n_2 \frac{\mu_0 a}{16\pi}\left(ln\tfrac{a}{\varepsilon}+2\right) I_0 \omega_c \, cos(\omega_c t) \tag{28}$$

Depending on the angular velocity of the current in the outer inductor, we can achieve a total emf_t value that is higher or lower than the value of a motional emf_m. However, our goal is to increase the induced voltage produced by the displacement of the membrane. Then, we can choose ω_c that will result at a multiplication factor greater than 2. In the case shown by Fig. 7 we can reach an emf_T voltage 3 times higher than the emf_m with two harmonic signals, the first have an angular velocity at ω_c-$2\omega_p$ and the second at ω_c+$2\omega_p$. This was done for a displacement of 20 µm, f_p=*1 kHz* and f_c=*10 kHz*. We can pass the resulting wave through a band-stop filter, to recuperate the original signal

proportional to the membrane deflection, permitting only the angular velocity of ω_c-2ω_p and/or ω_c+2ω_p and rejecting the others.

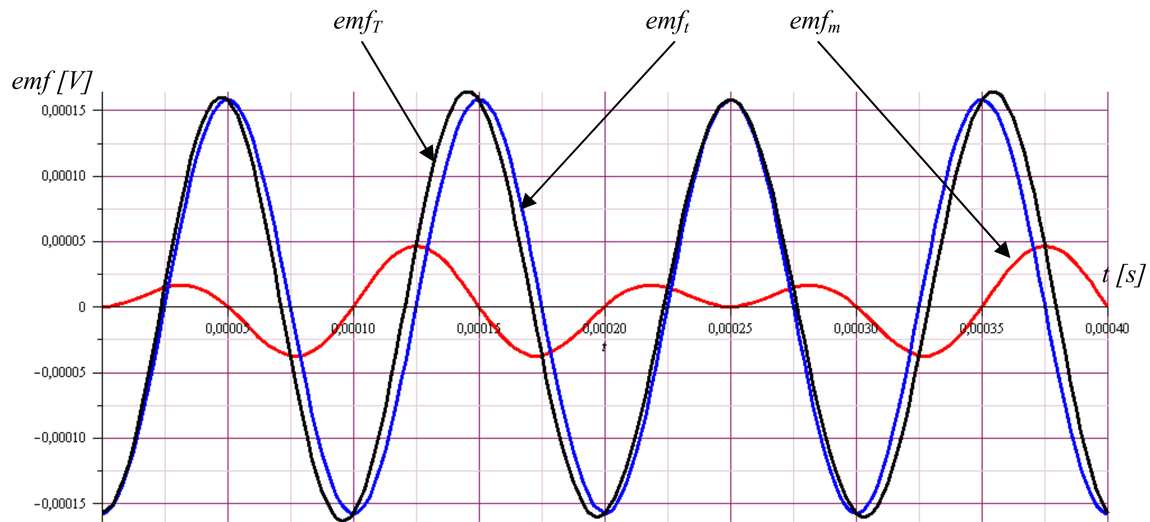

Fig. 7. Voltage form result, emf_T, of the sum of the emf_t and the emf_m.

4. Use of the Dual-layer Spiral Inductor

To improve the *emf* produced by the internal inductor and also to enhance the B-field we can use the symmetric dual-layer spiral inductor, structure shown in Fig. 8. Mutual inductance between adjacent spirals increases the total inductance of the multi-layer spiral inductor. In comparison with the conventional single-layer spiral inductors, theory and measurements show that, for a given silicon area, the dual-layer inductor provides the inductance value nearly three times higher than that of the single-layer inductor [22, 23]. The use of this kind of inductance structure in our microphone structure can lead to an *emf* which is four times higher than that given in the Equation 10. This can easily be seen since the number of inductor segments has been multiplied by two for both inductors.

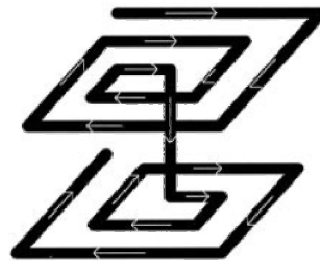

Fig. 8. Symmetric dual-layer spiral inductor structure.

5. Conclusion

We have shown a new structure of a monolithic CMOS integrated inductive microphone. It is based on the variation of the mutual inductance between an outer fixed inductor and an inner suspended inductor. This inner inductor is designed on a suspended membrane attached with four arms. Detailed electromagnetic modeling and calculation was done to find solutions leading to the increase of the

induced voltage gained in the inner inductor. A prototype chip fabrication of this inductive microphone has been done in a CMOS compatible process using a 0.6 μm technology. The electromagnetic study shows that the use of an AC current in the primary fixed inductor gives a larger induced voltage in the inner inductor. The induced voltage evaluated, in the μV range using a DC current solution, is found to be multiplied by a factor of 3 to 6 when using the alternative current. The output voltage of the electrodynamic microphone that achieves the μV range can be increased by the use of the symmetric dual-layer spiral inductor structure.

References

[1]. P. R. Scheeper, B. Nordstrand, J. O. Gullov, B. Liu, T. Clausen, L. Midjord, T. Storgaard-Larsen, A new measurement based on MEMS technology, *Journal of Microelectromechanical Systems,* 12, 2003, pp. 880–891.

[2]. J. Bay, O. Hansen, S. Bouwstra, Design of a silicon microphone with differential read-out of a sealed double parallel-plate capacitor*, Sensors and Actuators A*, 53, 1996, pp. 232–236.

[3]. D. P. Arnold, T. Nishida, L. N. Cattafesta, M. Sheplak, A directional acoustic array using silicon micromachined piezoresistive microphones, *Journal of the Acoustical Society of America,* 113, 1, 2003, pp. 289–298.

[4]. Gang Li, Yitshak Zohar and Man Wong, Piezoresistive microphone with integrated amplifier realized using metal-induced laterally crystallized polycrystalline silicon, *Micro Electro Mechanical Systems, 2004. 17th IEEE International Conference on MEMS*, pp. 548- 551.

[5]. S. B. Horowitz, T. Nishida, L. N. Cattafesta III and M. Sheplak, Design and Characterization of a Micromachined Piezoelectric Microphone, *11th AIAA/CEAS Aeroacoustics Conference (26th AIAA Aeroacoustics Conference)*, 23 - 25 May 2005, Monterey, California.

[6]. R. Kessmann, M. Klaiber, and G. Hess, Silicon condenser microphones with corrugated silicon oxide/nitride electret membranes, *Sens. Actuators A, Phys.,* Vol. 100, No. 2/3, Sep. 2002, pp. 301–309.

[7]. S. T. Hansen, A. S. Ergun, W. Liou, B. A. Auld, and B. T. Khuri-Yakub, Wideband micromachined capacitive microphones with radio frequency detection, *J. Acoust. Soc. Amer*., Vol. 116, No. 2, Aug. 2004, pp. 828–842.

[8]. Bilaniuk N, Optical microphone transduction techniques, *Applied Acoustics*, Vol. 50, No. 1, January 1997, pp. 35-63(29).

[9]. Håkon Sagberg, Aasmund Sudbø, Olav Solgaard, Kari Anne Hestnes Bakke, and Ib-Rune Johansen Optical Microphone Based on a Modulated Diffractive Lens, *IEEE Photonics Technology Letters*, Vol. 15, No. 10, October 2003.

[10].N. A. Hall, B. Bicen, M. K. Jeelani, W. Lee, S. Qureshi, and F. L. Degertekin, Micromachined microphones with diffraction-based optical displacement detection, *J. Acoust. Soc. Amer*., Vol. 118, No. 5, Nov. 2005, pp. 3000–3009.

[11].F. Tounsi, B. Mezghani, S. Smaoui, M. B. Jallouli, N. Ghamgui, M. Masmoudi, Acoustical electrical modeling of CMOS integrated micromachined inductive microphone, *European Micro and Nano systems EMN'04*, 20-21 October 2004, Paris, France.

[12].F. Tounsi, L. Rufer, B. Mezghani, M. Masmoudi and S. Mir, Electromagnetic modeling of an integrated micromachined inductive microphone, *4th IEEE International Conference on Design & Test of Integrated Systems in Nanoscale Technology (IEEE DTIS '2009),* April 6-10, 2009, Cairo, Egypt.

[13].William H. Hayt, John A. Buck, Engineering Electromagnetics, 6th Edition, *Mcgraw Hill* Series in Electrical and Computer Engineering, Chapter 10, pp. 320-347.

[14].Sunderarajan S. Mohan, C. Patrick Yue, Maria del Mar Hershenson, S. Simon Wong and Thomas H. Lee, Modeling and characterization of on-chip transformers, *IEEE International Electron Devices Meeting (IEDM)*, December 6-9, 1998.

[15].S. S. Mohan, The design, modeling and optimization of on-chip inductor and trans-former circuits, *Ph. D Dissertation*, Stanford University, Stanford, 1999.

[16].F. Tounsi, M. B. Jallouli, B. Mezghani, S. Smaoui, N. Ghamgui and M. Masmoudi, CMOS integrated micromachined inductive microphone, *International Conference on Microelectronics (ICM 2004)*, 6-8 December 2004, Tunis, Tunisia.

[17]. H. M. Greenhouse, Design of planar rectangular microelectronic inductors, *IEEE Trans. Parts, Hybrids, Packaging*, Vol. PHP-10, June 1974, pp. 101-109.
[18]. F. W. Grover, Inductance Calculations, *Dover,* New York, 1946.
[19]. Jenei S., Nauwelaers B. K. J. C., Decoutere S., Physics-based closed-form inductance expression for compact modeling of integrated spiral inductors, *IEEE Journal of Solid-State Circuits*, Vol. 37, Issue 1, Jan 2002, pp. 77 – 80.
[20]. C. P. Yue, S. S. Wong, Physical modeling of spiral inductors on silicon, *IEEE Transactions on Electron Devices*, Vol. 47, Issue 3, March 2000, pp. 560–568.
[21]. Tai L. Chow, Introduction to Electromagnetic Theory: A Modern Perspective, Chapter 4, pp. 126-170.
[22]. Pan, S. J., L. W. Li, and W. Y. Yin, Compact equivalent circuit model of two-layer spiral inductors, *International Journal of RF and Microwave Computer-Aided Engineering*, Vol. 13, No. 2, 2003, pp. 148–153.
[23]. Y. K. Koutsoyannopoulos and Y. Papananos, Systematic analysis and modeling of integrated inductors and transformers in RF IC design, *IEEE Trans Circuits Systems II Analog Digital Signal Process,* 47, 2000, pp. 699–713.

2009 Copyright ©, International Frequency Sensor Association (IFSA). All rights reserved.
(http://www.sensorsportal.com)

Guide for Contributors

Aims and Scope

Sensors & Transducers Journal (ISSN 1726-5479) provides an advanced forum for the science and technology of physical, chemical sensors and biosensors. It publishes state-of-the-art reviews, regular research and application specific papers, short notes, letters to Editor and sensors related books reviews as well as academic, practical and commercial information of interest to its readership. Because it is an open access, peer review international journal, papers rapidly published in *Sensors & Transducers Journal* will receive a very high publicity. The journal is published monthly as twelve issues per annual by International Frequency Association (IFSA). In additional, some special sponsored and conference issues published annually. *Sensors & Transducers Journal* is indexed and abstracted very quickly by Chemical Abstracts, IndexCopernicus Journals Master List, Open J-Gate, Google Scholar, etc.

Topics Covered

Contributions are invited on all aspects of research, development and application of the science and technology of sensors, transducers and sensor instrumentations. Topics include, but are not restricted to:

- Physical, chemical and biosensors;
- Digital, frequency, period, duty-cycle, time interval, PWM, pulse number output sensors and transducers;
- Theory, principles, effects, design, standardization and modeling;
- Smart sensors and systems;
- Sensor instrumentation;
- Virtual instruments;
- Sensors interfaces, buses and networks;
- Signal processing;
- Frequency (period, duty-cycle)-to-digital converters, ADC;
- Technologies and materials;
- Nanosensors;
- Microsystems;
- Applications.

Submission of papers

Articles should be written in English. Authors are invited to submit by e-mail editor@sensorsportal.com 8-14 pages article (including abstract, illustrations (color or grayscale), photos and references) in both: MS Word (doc) and Acrobat (pdf) formats. Detailed preparation instructions, paper example and template of manuscript are available from the journal's webpage: http://www.sensorsportal.com/HTML/DIGEST/Submition.htm Authors must follow the instructions strictly when submitting their manuscripts.

Advertising Information

Advertising orders and enquires may be sent to sales@sensorsportal.com Please download also our media kit:
http://www.sensorsportal.com/DOWNLOADS/Media_Kit_2009.pdf

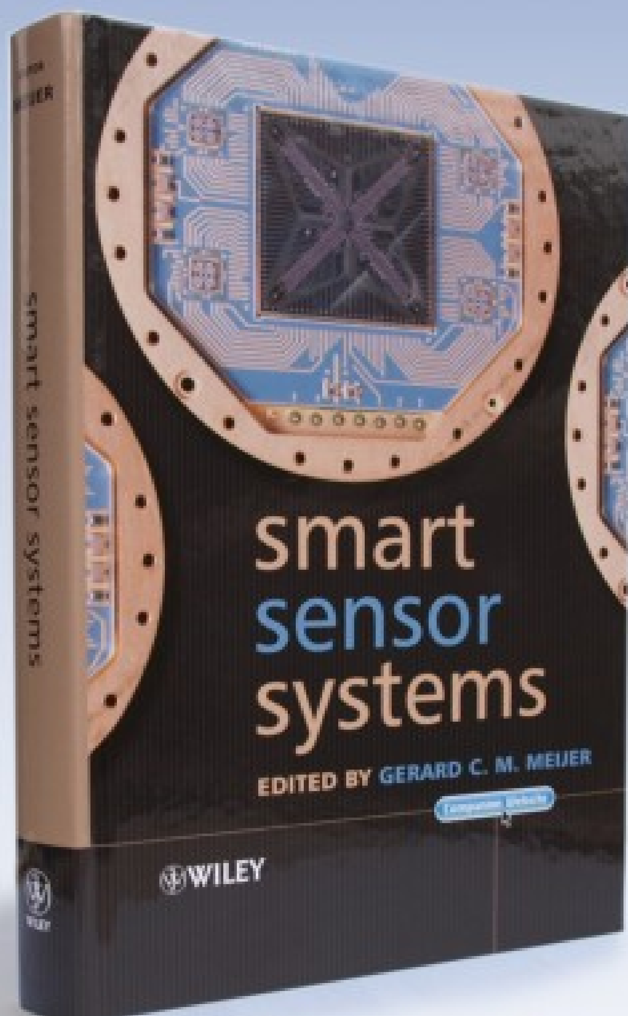

'Written by an internationally-recognized team of experts, this book reviews recent developments in the field of smart sensors systems, providing complete coverage of all important systems aspects. It takes a multidisciplinary approach to the understanding, design and use of smart semsor systems, their building blocks and methods of signal processing.'

Order online:
http://www.sensorsportal.com/HTML/BOOKSTORE/Smart_Sensor_Systems.htm

www.sensorsportal.com